ISSN: 2319-5967
ISO 9001:2008 Certified
International Journal of Engineering Science and Innovative Technology (IJESIT)
Volume 8, Issue 2, March 2019

Formation and Characterization of Ga_2O_3 nanofiber by electrospinning

Young Hun Km[a,b], Chang Sub Kim[a], Han Sol Back[a], Jeong Ju Baek[a], Ki Cheol Chang[a,], Gyo Jic Shin[a], Kyung Ho Choi[a,*]

[a] Intelligent Sustainable Material R&D Group, Korea Institute of Industrial Technology , Chenonan-si,31056, South Korea

[b] Department of chemical and Biomolecular Engineering, Yonsei University, Seoul, 03722, Korea

Abstract: ***β-Ga_2O_3 nanofibers were formed using a $Gacl_3$, PVP and deionized water solution via an electrospinning method. The as-electrospun amorphous nanofibers turned into polycrystalline nanofibers of monoclinic phase after annealing at 900˚C for 6hr. Material properties of the nanofibers were investigated using XRD and SEM. In addition, optical properties of sample was measured via the direct-bang gap model. The results indicated that the formed 1-dimentioinal β-Ga_2O_3 nanofiber could be applied to power devices (rather than a conventional 3-dimentioinal β-Ga_2O_3 substrate) to effectively remove the heat generated during device operation and thereby enhance device performance and reliability.***

Keywords: **Sol-gel, Beta-gallium oxide, wide-band gap semiconductors, electro spinning.**

I. BACKGROUND

β-Ga_2O_3 has received much attention in recent years because of wider-bandgap properties with the recent breakthrough of the single-crystal growth of β-Ga_2O_3 [1, 2], which offer significant economic benefit in various areas. β-Ga_2O_3 is a monocline crystal and transparent oxides in the visible spectrum down to ultraviolet (UV). It is getting more attention in the power devices [3, 4], deep-UV photodetectors [5] and light-emitting diodes (LEDs) [6]. The higher breakdown electric field of β-Ga_2O_3 than SiC and GaN makes β-Ga_2O_3 more attractive for power devices as shown in Fig. 1(a). The electrical performance of the commercially available Si-based power devices was also presented at the right-top as the solid circles in Fig. 1(a), whose device performance is limited by the inherent material property of Si substrate. To enhance the device efficiency, Si-based power devices need to be replaced by WBS such as SiC and GaN. For the power devices that carry high-current densities and modulate high-voltages, high thermal conductivity is a necessary material property to effectively dissipate a heat that is generated during the device operation. Despite the attractive electric properties of β-Ga_2O_3, it suffers from a low thermal conductivity of 13 $Wm^{-1}K^{-1}$ [7], compared to other WBS such as GaN (~150-200 $Wm^{-1}K^{-1}$) [8] and SiC (360-400 $Wm^{-1}K^{-1}$) [9] as shown in Fig. 1(b). This poor thermal conductivity of β-Ga_2O_3 tends to degrade device reliability and limit an operation region, and is also necessary to be accompanied by a bulky and heavy cooling system. To compensate this poor thermal conductivity of β-Ga_2O_3, a way to enhance a heat dissipation of β-Ga_2O_3 was recently reported via adopting lower dimension of materials [3]. In detail, the surface of a material is involved in the heat conduction process, so the heat transfer rate is

ISSN: 2319-5967
ISO 9001:2008 Certified
International Journal of Engineering Science and Innovative Technology (IJESIT)
Volume 8, Issue 2, March 2019

expected to be directly proportional to the surface area through which the heat is being conducted. In that sense, 1-dimentiional (1D) form of a material followed by 2D and 3D is desirable for efficient heat dissipation during the device operation. In fact, 2D nano-membrane of β-Ga_2O_3 was prepared using mechanical exfoliation method, but little attention has been paid to the 1D nanofibers of β-Ga_2O_3 in the range of few-tens nm [3].

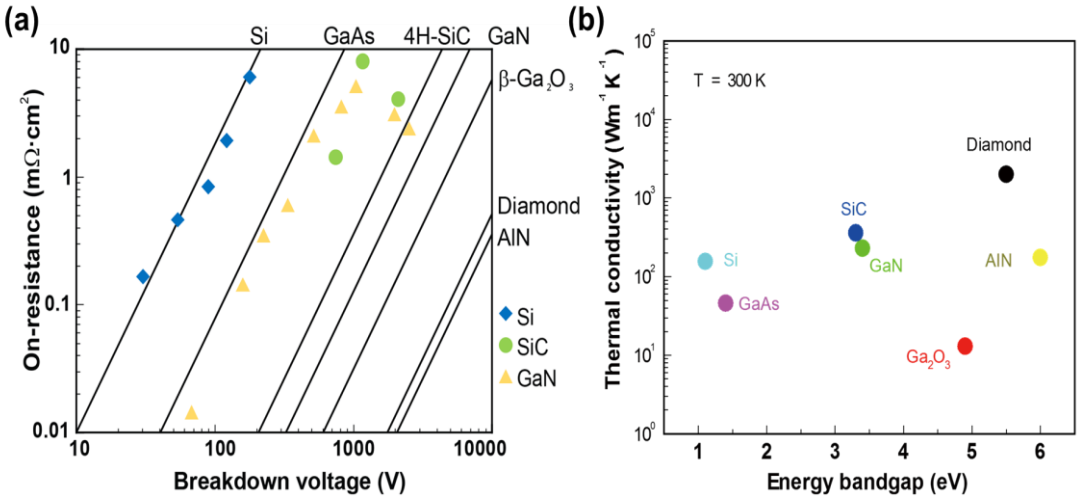

Fig. 1 (a) Theoretical limits of on-resistances of various WBS including Si as a function of break voltage [4, 10] (The solid circles at the right-top represent the commercially available Si devices) and (b) thermal conductivity with respect to the energy bandgap of various WBS including Si. [11-14].

In this work, we formed and characterized the electrospun β-Ga_2O_3 nanofibers at various annealing temperatures. The formation, morphology, and crystallinity of the nanofibers were analyzed using scanning electron microscopy (SEM), X-ray diffraction (XRD) and X-ray photoelectron spectroscopy (XPS). Finally, the optical bandgap of material at various annealing temperatures was extracted from the transmittance spectra via direct bandgap modeling.

II. METHODS

$GaCl_3$ (Aldrich, USA) and polyvinylpyrrolidone (PVP, MW=40,00,000; Duksan, Korea) were commercially obtained to form electrospun β-Ga_2O_3 nanofibers. Synthesis conditions were as follows: a 0.5 mol $GaCl_3$ was dissolved in a polyvinylpyrrolidone (PVP, MW=40,00, 000; Duksan, Korea) concentration of 0.1g/mL and the solution was continuously stirred for 24 hr before electrospinning. The electrospinning apparatus consisted of a syringe pump, a gauge metal needle, a grounded collector and a high voltage supply equipped with current and voltage digital meters. The solution was placed in a 5-mL syringe attached to the syringe pump and was fed into the metal needle at a flow rate of 0.1 μL/h. A high-voltage of 25 kV was applied between the needle and the ground of an aluminum foil with the distance of 8 cm. The formed electrospun- nanofibers were dried at room temperature for 24 hr, and subsequently annealed at 500, 700, and 900 ˚C for 6 hr, respectively. The morphology and diameters of the nanofibers annealed at various temperatures were characterized using SEM after Au coating of a few-nm thickness. The crystal structure and chemical state of the nanofibers depending on various annealing temperature was investigated using XRD and XPS respectively. Lastly, the nanofibers were

ISSN: 2319-5967
ISO 9001:2008 Certified
International Journal of Engineering Science and Innovative Technology (IJESIT)
Volume 8, Issue 2, March 2019

seated on single crystal quartz and optical bandgap of nanofibers at various annealing temperature was evaluated by transmittance spectra. To extract the energy bandgap of semiconductor, the expression of $(\alpha h\nu)^m$ versus hν is used, where m is an integer or semi-integer, α is the absorption coefficient, h is the Planck constant, and ν is the frequency of the electromagnetic radiation [15, 16]. For the β-Ga_2O_3 semiconductor, m=2 was used because the electron assumed to directly transit from the valence to the conduction band [3].

III. RESULTS

A. Formula and Equation

$T = [(1-R)^2\exp(-\alpha d)]/[1-R^2\exp(-2\alpha d)]$

$\alpha = -(1/d)\ln(T)A^*(E-Eg)$

Where α, d, T, A^*, E and Eg are adsorption coefficient, film thickness, transmittance, constant that does not depend on hv, photon energy (hv), and indirect band gap (eV), respectively.

B. Figures and Tables

The morphology of nanofibers annealed at various temperatures was presented in Fig. 2 via SEM. The as-electrospun nanofiber showed a continuous morphology and their continuity remain even at 900 ˚C. However, the diameter of the nanofibers decrease with the annealing temperatures, which was attributed to the removal of the organic residues and the structural densification. This SEM result would be correlated with XRD and XPS analysis.

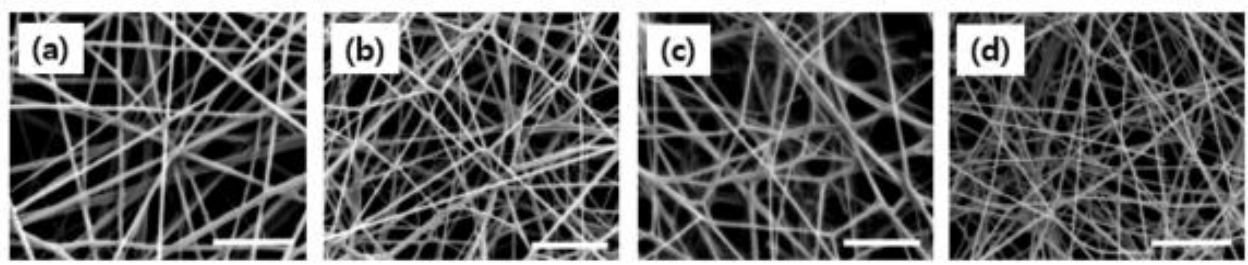

Fig. 2 Nanofiber SEM images (a) as-electrospun, annealed at (b) 500 ˚C, (c) 700 ˚C, and (d) 900 ˚C for 6 hr. The scale bar is 1 μm.

The diameter distribution depending on various annealing temperatures was further quantified in Fig. 3. This shows that the nanofibers with diameters of around 60 nm were formed with the solution via electrospinning method. The nanofiber diameters decreased continuously with the annealing temperatures until reaching approximately 30 nm at 900 ˚C.

The crystal structures of the nanofibers via XRD are presented in Fig. 4. The results showed that no distinct peak was observed for the as-electrospun nanofibers (data not shown), indicating that an amorphous phase had formed via the electrospinning method. This amorphous phase turned into a polycrystalline structure after annealing at 500 ˚C. As the annealing temperature increased up to 900 ˚C, the typical β-Ga_2O_3 peak became dominant. The grain size of the nanofibers also increased from 0.07 nm (500 ˚C) to 0.12 nm (700 ˚C) and 0.37 nm (900 ˚C), which was measured via the Scherrer method [17]

ISSN: 2319-5967
ISO 9001:2008 Certified
International Journal of Engineering Science and Innovative Technology (IJESIT)
Volume 8, Issue 2, March 2019

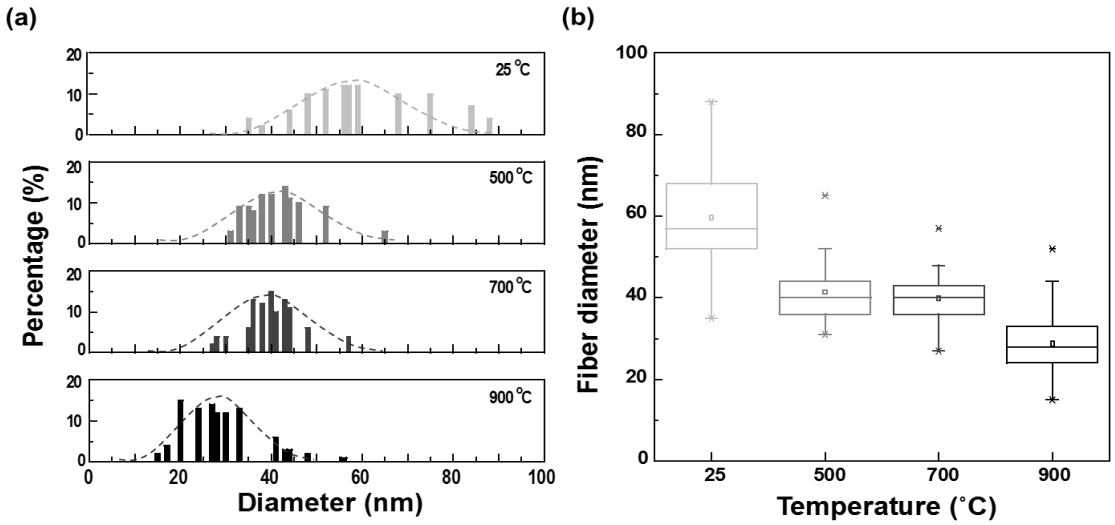

Fig. 3 (a) Diameter distribution histograms of nanofibers annealed at various temperatures. (b) Nanofiber diameter distribution as a function of annealing temperatures.

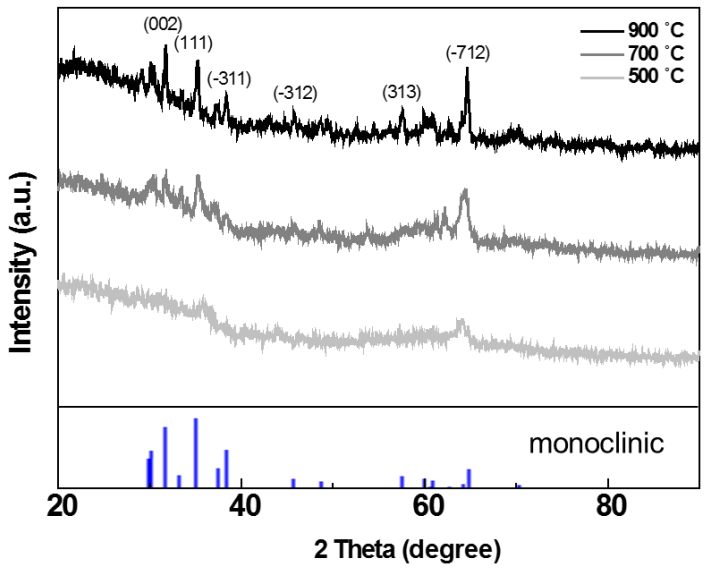

Fig. 4 XRD patterns of the Ga_2O_3 nanofibers at different annealing temperatures, and as per standard patterns of different Ga_2O_3 structures.

The chemical states of the nanofibers via XPS are presented in Fig. 5. The results in Fig. 5(a) showed that the as-electrospun nanofibers possessed C-O and C=O bonds beside the C-C bond. As seen in Fig. 5(b), additional C-O and C=O bonds were also exhibited along with Ga-O bond. In addition, significant Cl-residues remained in the as-electrospun nanofibers. The amorphous nanofibers containing Cl, however, turned into Cl-free crystal nanofibers through the high annealing process. Thus, the nanofibers annealed at 900 ˚C represented typical β-Ga_2O_3 chemical states.

ISSN: 2319-5967
ISO 9001:2008 Certified
International Journal of Engineering Science and Innovative Technology (IJESIT)
Volume 8, Issue 2, March 2019

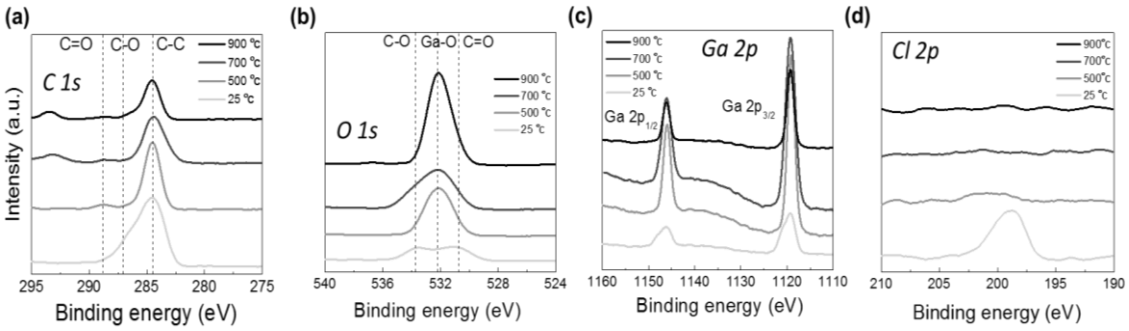

Fig. 5 XPS spectra of the nanofibers annealed at various temperatures. (a-d) The C1s, O1s, Ga 2p, and Cl 2p scan, respectively, of the four different nanofibers [18-20]

Finally, the optical bandgap of the nanofibers at different annealing temperatures was extracted via transmittance spectra. The plot of the $(\alpha hv)^m$ as a function of hv in Fig. 6(b) was obtained from the transmittance curve in Fig. 6(a). The results showed that the optical bandgap of the nanofibers increased with annealing temperature until reaching 4.75 eV at 900 ˚C. This was comparable to the reported value of 4.9 [3]. The minor discrepancy was attributed to the scattering in the polycrystalline structure.

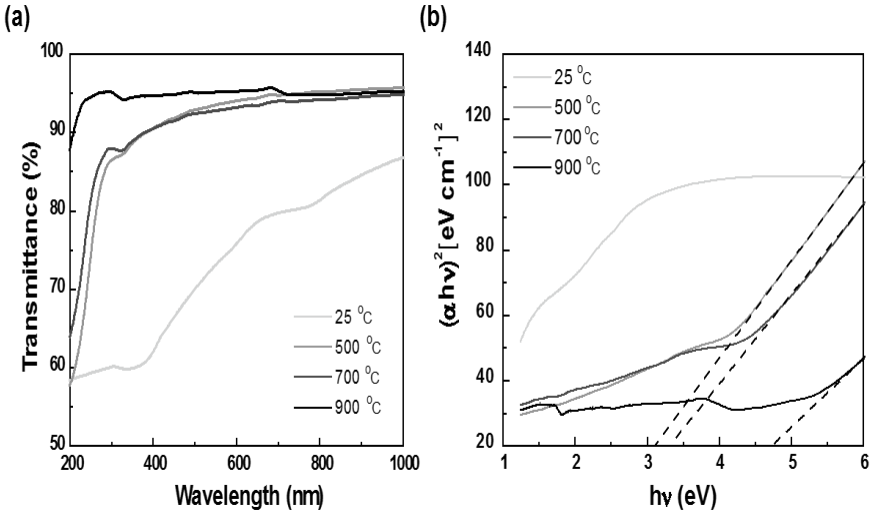

Fig. 6 (a) Transmittance and (b) optical energy bandgap at different annealing temperatures.

C. CONCLUSION

β-Ga_2O_3 nanofibers were formed using a $GaCl_3$ and PVP solution and the electrospinning method. The electrospun nanofibers were characterized via SEM, XRD, XPS, and transmittance analyses. It was determined that the amorphous as-electrospun nanofibers turned into monoclinic polycrystal nanofibers at 900 ˚C annealing. In addition, the Cl and C residues in the as-electrospun nanofibers were removed, and the diameters of the nanofibers decreased as the annealing temperatures increased. The optical bandgap of the nanofibers was measured to be 4.75 eV via the direct-bandgap model. It was concluded that the formed β-Ga_2O_3 nanofibers could be applied to power devices to effectively remove the heat generated during device operation, which would enhance device performance.

ISSN: 2319-5967
ISO 9001:2008 Certified
International Journal of Engineering Science and Innovative Technology (IJESIT)
Volume 8, Issue 2, March 2019

REFERENCES

[1] Galazka, Z.; Uecker, R.; Irmscher, K.; Albrecht, M.; Klimm, D.; Pietsch, M.; Brützam, M.; Bertram, R.; Ganschow, S.; Fornari, R. Czochralski (2010). Growth and characterization of β-Ga_2O_3 single crystals. Cryst. Res. Technol., 45(2), 1229-1236.

[2] M. Higashiwaki, K. Sasaki, A. Kuramata, T. Masui, Yamakoshi, Gallium oxide (Ga_2O_3) metal-semiconductor field-effect transistors on single-crystal β- Ga_2O_3 (010) substrates, S.

[3] Hwang, W. S.; Verma, A.; Peelaers, H.; Protasenko, V.; Rouvimov, S.; Xing, H.; et al.. & Albrecht, M. (2014). High-voltage field effect transistors with wide-bandgap β-Ga2O3 nanomembranes. Appl. Phys. Lett., 104, 203111.

[4] Higashiwaki, M.; Sasaki, K.; Wong, M. H.; Kamimura, T.; Krishnamurthy, D.; Kuramata, A.; Masui, T.; Yamakoshi, S.(2013) Depletion-mode Ga_2O_3 MOSFETs on β-Ga_2O_3 (010) substrates with Si-ion-implanted channel and contacts. In Electron Devices Meeting (IEDM). **2013**, pp 28-7.

[5] Oshima, T.; Okuno, T.; & Fujita, S. Ga2O3 thin film growth on c-plane sapphire substrates by molecular beam epitaxy for deep-ultraviolet photodetectors. JPN. J. of Appl. Phys. **2007**, 46, 7217-7220.

[6] Kim, C. J.; Kang, D.; Song, I.; Park, J. C.; Lim, H.; Kim, S.; Lee, E.; Chung, R.; Lee, J. C.; Park, Y. Highly stable Ga2O3-In2O3-ZnO TFT for active-matrix organic light-emitting diode display application. In Electron Devices Meeting (IEDM). **2006**, (pp. 1-4). IEEE.

[7] Víllora, E. G.; Shimamura, K.; Ujiie, T.; Aoki, K. Electrical conductivity and lattice expansion of β-Ga 2 O 3 below room temperature. Appl. Phys. Lett. **2008**, 92, 202118.

[8] C. Mion, Thesis, (2005) North Carolina State University.

[9] Glassbrenner, C. J.; & Slack, G. A. (1964) Thermal conductivity of silicon and germanium from 3 K to the melting point. Am. Phys. Soc.134, A1058.

[10] Zhao, J.; Zhang, W.; Xie, E.; Ma, Z.; Zhao, A.; Liu, Z. (2011) Structure and photoluminescence of β-Ga 2 O 3: Eu 3+ nanofibers prepared by electrospinning. App. Surf. Sci, 257, 4968-4972.

[11] Ikeda, N.; Kaya, S.; Li, J.; Sato, Y.; Kato, S.; Yoshida, S. (2008) High power AlGaN/GaN HFET with a high breakdown voltage of over 1.8 kV on 4 inch Si substrates and the suppression of current collapse. Proceedings of the 20th International Sym. On Power Semicon. Dev. & IC's, Oralando, FL, May 18-22, 287-290.

[12] Holland, M. G. (1964) Phonon scattering in semiconductors from thermal conductivity studies. Phys. Re, 134, A471.

[13] Che, J.; Çağın, T.; Deng, W.; Goddard III, W. A. (2000) Thermal conductivity of diamond and related materials from molecular dynamics simulations. J. of Chem. Phys, 113, 6888-6900.

[14] Jackson, T. B.; Virkar, A. V.; More, K. L.; Dinwiddie, R. B.; Cutler, R. A. (1997) High-Thermal-Conductivity Aluminum Nitride Ceramics: The Effect of Thermodynamic, Kinetic, and Microstructural Factors. J. Am Ceram.

ISSN: 2319-5967
ISO 9001:2008 Certified
International Journal of Engineering Science and Innovative Technology (IJESIT)
Volume 8, Issue 2, March 2019

Soc, 80, 1421-1435.

[15] Madelung, O. (1981) Introduction to Solid State Theory, Springer Series in Solid State Sciences, Springer: Berlin, Volume 2, pp. 270.

[16] Smith, R. A. (1978) Semiconductors, Cambridge University Press: Cambridge, pp. 315.

[17] Klug, H.P.; Alexander, L. E (1954) X-ray diffraction procedures, Wiley: New York, USA, Volume 2, pp. 163-210.

[18] Dwivedi, N.; Yeo, R. J.; Satyanarayana, N.; Kundu, S.; Tripathy, S.; Bhatia, C. S. (2015) Understanding the role of nitrogen in plasma-assisted surface modification of magnetic recording media with and without ultrathin carbon overcoats. Sci Rep,5, 7772:1-7772:13.

[19] Sul, Y. T. (2010) electrochemical growth behavior, surface properties, and enhanced in vivo bone response of TiO. Int. J. Nanomedicine., 5, 87-100.

[20] Lopez, I.; Utrilla, A. D.; Nogales, E.; Mendez, B.; Piqueras, J.; Peche, A.; Ramírez-Castellanos, J.; González-Calbet, J. M.(2012) In-doped gallium oxide micro-and nanostructures: morphology, structure, and luminescence properties. J. Phys. Chem. C, 116, 3935-3943.